Review

A practical and systematic review of Weibull statistics for reporting strengths of dental materials

Janet B. Quinn, George D. Quinn*

ADAF Paffenbarger Research Center, National Institute of Standards and Technology, Gaithersburg, MD, USA

ARTICLE INFO

ABSTRACT

Objectives. To review the history, theory and current applications of Weibull analyses sufficient to make informed decisions regarding practical use of the analysis in dental material strength testing.

Data. References are made to examples in the engineering and dental literature, but this paper also includes illustrative analyses of Weibull plots, fractographic interpretations, and Weibull distribution parameters obtained for a dense alumina, two feldspathic porcelains, and a zirconia.

Sources. Informational sources include Weibull's original articles, later articles specific to applications and theoretical foundations of Weibull analysis, texts on statistics and fracture mechanics and the international standards literature.

Study selection. The chosen Weibull analyses are used to illustrate technique, the importance of flaw size distributions, physical meaning of Weibull parameters and concepts of "equivalent volumes" to compare measured strengths obtained from different test configurations.

Conclusions. Weibull analysis has a strong theoretical basis and can be of particular value in dental applications, primarily because of test specimen size limitations and the use of different test configurations. Also endemic to dental materials, however, is increased difficulty in satisfying application requirements, such as confirming fracture origin type and diligence in obtaining quality strength data.

* Corresponding author at: ADAF, Stop 854-6, National Institute of Standards and Technology, Gaithersburg, MD 20899, USA.
Tel.: +1 301 975 5765.
E-mail address: george.quinn@nist.gov (G.D. Quinn).

Contents

1.   Introduction

This paper reviews Weibull statistics in order to facilitate informed decisions regarding practical use of the analysis as it applies to dental material strength testing. Weibull statistics are commonly used in the engineering community, but to a somewhat lesser extent in the dental field where applicability has been questioned [1,2]. A possible confusing factor is that Waloddi Weibull originally presented his analyses partially on empirical grounds; published theoretical confirmation was not available until many years later. Even as a theoretical basis was being constructed, Weibull, as an engineer, seemed more concerned with what worked [3,4]. In order to assess applicability to the specific field of dental material strength testing, it is helpful to start with a brief history and overview of basic concepts of extreme value theory, fracture mechanics, and flaw populations as they pertain to the theoretical foundation of Weibull analysis.

1.1.   Background: brittle failure prediction, fracture mechanics and flaws

It is often noted that dental restorative ceramics and composites, while popular in terms of esthetics and biocompatibility, are susceptible to brittle fracture. This type of failure is particularly difficult to predict. Imminent brittle fracture is seldom preceded by warning, such as visible deformation, nor do seemingly identical brittle components appear to break at the same applied stress. Ductile materials deform to evenly distribute stresses throughout a region, but in stiff, brittle materials, stress concentrations at specimen geometry changes, cracks, surface irregularities, pores and other intrinsic flaws are not relieved. Hence the design methodologies and test methods for ductile materials are unsuitable for brittle materials and different test methods and design approaches are needed.

A series of catastrophic events, often epitomized by the Liberty ship [5] and Comet airplane [6] disasters, spectacularly demonstrated the inapplicability of ductile strength testing analyses to brittle failure prediction. Such disasters spurred the development of the science of fracture mechanics in order to understand the conditions of failure through crack growth rather than by ductile mechanisms [7].

In the early 1920s, Griffith postulated that crack extension in brittle materials occurs when there is sufficient elastic strain energy in the vicinity of a growing crack to form two new surfaces [8]. In the 1950s Irwin built on Griffith's work to associate crack extension with an "energy release rate" [9]. This led to a new parameter, K_{Ic}—fracture toughness, or resistance to crack growth. Irwin's approach enabled strength predictions based on fracture toughness calculations that relate crack extension to the sizes of preexisting cracks or "flaws" within a material. For the most common case of a small flaw in a far field tensile stress field, modern fracture mechanics relates the applied fracture stress at the fracture origin, σ_f, to a flaw size, c [7]:

$$\sigma_f = \frac{K_{Ic}}{Y\sqrt{c}} \tag{1}$$

where Y is a dimensionless, material-independent constant, related to the flaw shape, location and stress configuration and is called the stress intensity shape factor. "Flaws" are not necessarily inadvertent defects or blemishes in a material. No material is perfectly homogenous, and all contain some sort of discontinuities on some scale. These discontinuities might be pores, inclusions, distributed microcracks associated with grain boundaries or phase changes during processing, regions of dislocations or slight variations of chemistry, or many other possible variants and combinations. They could also be surface distributed flaws such as grinding cracks. Flaws in this sense are intrinsic to the material or the way it was shaped or processed, and are distributed in some way throughout the material surface or volume. It can be seen from the equation that the smallest strengths are associated with the largest flaw sizes.

The idea of failure being associated with a largest flaw, or "weakest link theory", is not recent. Leonardo DaVinci is reputed to have conducted tests *circa* 1500 involving baskets suspended by different lengths of wire of nominally identical diameter [10]. DaVinci gradually filled the baskets with sand and noted the baskets suspended by shorter wires could hold more sand, an outcome that is expected if it is assumed that there is a lower probability of encountering a large flaw in a shorter wire. DaVinci did not know exactly where a particular wire would break, but he recommended that multiple tests be done for each wire length, suggesting that there was a statistical variation in the strengths and failure locations of wires of a same length. Since DaVinci's time, much progress has been made both in our ability to identify critical flaw properties and in refining predictions based on weakest link theory and statistical failure probabilities.

1.2. Extreme value distributions of "largest flaws"

Suppose a material has a flaw size distribution such as the normal, or Gaussian, distribution illustrated in Fig. 1. Although the flaws have different sizes, suppose they are all of the same general type that initiate failure. Finally, suppose that small material test specimens are withdrawn from this parent population. Each test specimen will contain a discrete flaw population based on the parent distribution, and the largest flaw within the highly stressed regions of each test specimen will precipitate failure if uniform tension is applied.

If one is very unlucky, a randomly withdrawn material test specimen will contain an unusually large flaw, at the very end of the tail at the right of the parent distribution in Fig. 1. The test specimen will be very weak. If one is very fortunate, however, the largest flaw in a random material test specimen will not be far into the tail. This specimen will be relatively strong. If many random test specimens are withdrawn, most of them will contain a largest flaw that is somewhere within the parent population tail of large flaws. The "largest flaw" distribution might look like the shaded portion of Fig. 1.

The distribution of "largest flaws" of many withdrawn test specimens from a parent population is an example of an extreme value distribution. The "largest flaw" population is not expected to be a symmetric distribution, whether or not the parent population is Gaussian as in Fig. 1 example.

Suppose now that larger-sized test specimens of the same material are tested. Each of these physically larger test specimens contains more flaws than each of the smaller test specimens in the previous thought experiment. Since a larger test specimen contains more flaws, it is more likely to contain a very large flaw corresponding to the far right portion of the tail in Fig. 1 parent population. If many larger-sized test specimens are withdrawn, their "largest flaw" distribution will be weighted further to the right within the parent population tail than the previous "largest flaw" distribution of smaller test specimens. The "largest flaw" distributions "march to the right" as the physical sizes of the test specimen increase.

One result of "largest flaw" distributions that depend on the physical size of test specimens is that strength distributions, which are based on flaw sizes, will similarly depend on test specimen size. Strength distributions will inversely "march" left or right in accordance with "largest flaw" distributions in a mathematically predictable fashion. Also, strength distributions would not be expected to be symmetric if the "largest flaw" distributions are not symmetric.

Currently, many data in the dental literature are simply reported in terms of mean values with standard deviations calculated by assuming symmetric, normal strength distributions about an average. This assumption can still yield insight into material strengths and strength ranges. In fact, the assumed normal strength distribution may not greatly differ from an extreme value distribution in providing strength estimates of similarly sized and stressed test pieces. Unfortunately, such predictions only hold for the specific test specimen size and shape in the particular test configuration under laboratory conditions. As will be shown, besides more accurately characterizing material strength, extreme value statistics are a powerful tool that yield parameters that can be used to relate test strength data to expected strengths for different stress configurations, different test specimen sizes, and different testing conditions.

1.3. The Weibull distribution

Returning to Fig. 1, it can be seen that the parent distribution tail at the right is much more important than the rest of the parent distribution containing smaller flaws. Since small flaws in the test specimens do not precipitate failure, it does not matter how small these flaws are or how their sizes are distributed. The left side of the total flaw distribution in Fig. 1 has very little bearing on the "largest flaw" distribution.

The original total flaw population does not have to be normal or symmetric to result in an extreme value distribution shaped similar to the shaded portion in the figure. The right side of the parent flaw distribution, the tail of large flaws, dominates the shape of the "largest flaw" distribution. This is because only *one* very large flaw in a test specimen is necessary to be counted as "the largest flaw", but if the largest flaw is relatively small, *all* the other flaws in the test specimen have to be smaller. The distribution is thus skewed to the right as in Fig. 1, following the parent distribution tail. Extreme value distributions in general "follow the tail" [11]. Focusing only on
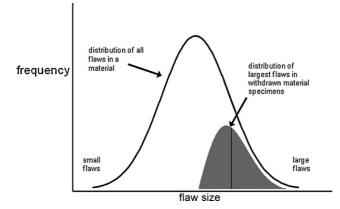

Fig. 1 – Total flaw distribution in a material (curved line). Withdrawing multiple test pieces from the total flaw population and collecting the largest flaw from each test piece results in a different distribution of "largest flaws" (shaded area).

the tails allows simple, generalized parametric functions to be used in extreme value statistical models. Such models have been defined to accommodate underlying distribution tails that deviate considerably from the Gaussian shape in Fig. 1 example.

There are three commonly recognized families of extreme value distributions [11–13] where $G(x)$ is the probability distributions function for an outcome being less than x for a sample set of n independent measurements:

Type I. Gumbel $G(x) = \exp(-\exp^{-(x-\mu)/\sigma})$ for all x

Type II. Fréchet : $G(x) \begin{cases} = \exp(-((x-\mu)/\sigma)^{-\xi}) & \text{for } x \geq \mu \\ = 0 & \text{otherwise} \end{cases}$

Type III. Weibull : $G(x) \begin{cases} = \exp(-((\mu-x)/\sigma)^{\xi}) & \text{for } x \leq \mu \\ = 1 & \text{otherwise} \end{cases}$

where μ, $\sigma(>0)$, and $\xi(>0)$ are the location, scale and shape parameters, respectively.

Fisher and Tippet [12] are credited [11,13] with defining the extreme value distributions in 1928, when they showed there could only be the three types. Some graphical examples of the probability density functions of the three types of extreme value distributions are shown in Fig. 2.

All three extreme value distributions have a theoretical basis for characterizing phenomena founded on weakest link theory. For strength dependency on an underlying material flaw distribution, the goodness-of-fit of any of the extreme value distributions depends on the shape of the flaw distribution tail. In this regard, Type III, or the Weibull distribution, is usually considered the best choice because it is bounded (the lowest possible fracture strength is zero), the parameters allow comparatively greater shape flexibility, it can provide reasonably accurate failure forecasts with small numbers of test specimens and it provides a simple and useful graphical plot [4,14]. In what has been hailed as his "hallmark paper" in 1951 [15], Weibull based the wide applicability of the distribution on functional simplicity, satisfaction of necessary boundary con-
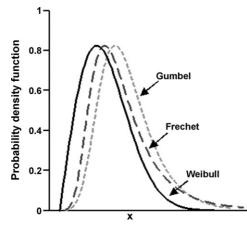

Fig. 2 – Probability density functions for the three extreme value distributions, arbitrarily placed along the abscissa (x) axis for easier shape comparison. Both the Weibull and Gumbel functions have demonstrated good fits for strengths of brittle materials, but a theoretical basis has been demonstrated for the Weibull distribution.

ditions and, mostly, good empirical fit. The parameter symbols and form of the extreme value functions are usually written differently for reliability analyses. In the specific case of Weibull fracture strength analysis, the cumulative probability function is written such that the probability of failure, P_f, increases with the fracture stress variable, σ:

$$P_f = 1 - \exp\left[-\left(\frac{\sigma - \sigma_u}{\sigma_\theta}\right)^m\right] \tag{2}$$

This is known as the Weibull three parameter strength distribution. The threshold stress parameter, σ_u, represents a minimum stress below which a test specimen will not break. The scale parameter or characteristic strength, σ_θ, is dependent on the stress configuration and test specimen size. The distribution shape parameter, m, is the Weibull modulus. This is the equation form that Weibull presented in his original publications, directly derived from weakest link theory [3]. He was conservative and disclaimed any theoretical basis, not because of misgivings concerning extreme value or weakest link theory, which was well established by then, but because he perceived it was "hopeless to expect a theoretical basis for distribution functions of random variables such as strength properties". Since Weibull's initial publications in 1939 and 1951, however, the science of fracture mechanics has enabled determinations of quantitative functional relationships between strength and flaws in brittle materials, as exemplified in Eq. (1).

By 1977, Jayatilaka and Trustrum [16] used fracture mechanics to develop a general expression for the failure probability using several general flaw size distributions suggested by experimental work. They coupled these flaw size distributions with the fracture mechanics criterion, Eq. (1), and integrated the risk of breakage over component volumes and then derived a number of different strength distributions [16,17]. Their derivations are too lengthy to repeat here and the reader is encouraged to review their exposition in the original references. They showed that the right side tail of many parent flaw size distributions such as shown in Fig. 1 often can be modeled by a simple power law function: $f(c) = \text{constant } c^{-n}$ where c is the flaw size. In such cases, the resulting strength distribution is the Weibull distribution with $m = 2n - 2$. Danzer et al. [18–20] have done similar derivations with more generalized flaw size distributions and have reached the same conclusions. Subsequent work, including painstaking measurement of flaw sizes and constructing distributions, has confirmed the power law function for the distribution of large crack sizes and hence the theoretical basis for the Weibull approach [21–23]. In other words, a reasonable power law distribution for large flaw sizes, classical fracture mechanics analysis, and weakest link theory lead directly to the Weibull strength distribution.

Today's engineers routinely utilize Weibull statistics for characterizing failure of brittle materials. Numerous and diverse studies in the engineering literature report data in terms of Weibull parameters where the strengths are related to fractographically determined flaw types and sizes [24–26]. Such studies substantiate the existence of flaw distributions that lead to strength distributions that can be modeled by Weibull statistics for a wide range of materials. As noted ear-

lier, fractographic examinations are becoming more common in relating flaw types and sizes to strengths of dental restoration materials [27–29]. While this shows that characterizing flaw populations in dental materials is possible, this does not prove it is easy or possible in every case. Many dental materials have rough microstructures, where it can be particularly difficult to identify fractographic features [30,31]. Also, it is not unusual to have multiple flaw types present which complicate the Weibull analysis.

Major standards organizations throughout the world have published specific guidelines for reporting ceramic strength in terms of Weibull parameters, including ASTM (C1239) [32], the Japanese Industrial Standards Organization (JIS R1625) [33], the European Committee for Standardization (CEN ENV 843) [34], and the International Organization for Standards (ISO 20501) [35]. These standards are very similar and use the identical Maximum Likelihood Estimation analysis to calculate the Weibull parameters. A newly revised (2008) Ceramic Material for Dentistry standard (ISO 6872) [36] is the sole exception and uses a simpler linear regression calculation in an informative annex.

Since many brittle materials used in structural engineering are also used in restorative dentistry, are Weibull analyses appropriate for ceramic dental materials? To answer this, the specific underlying assumptions and conditions inherent in applying Weibull statistics must be examined.

2. Considerations for using Weibull statistics for dental materials

A good data set is required for any credible property determination, and it can be deduced from the previous paragraphs that diligence in test specimen preparation and testing procedures is particularly important when using Weibull statistics. Test specimens breaking from inconsistent machining or handling, or haphazard alignment, are not representative of a specific flaw population, and do not contribute to a valid data set for Weibull analysis. A materials advisory board committee in 1980 [37] concluded that: "Ceramic strength data must meet stringent quality demands if they are to be used to determine the failure probability of a stressed component. Statistical fracture theory is based on the premise that specimen-to-specimen variability of strength is an intrinsic property of the ceramic, reflecting its flaw population and not unassignable measurement errors. Ceramic strength data must be essentially free of experimental error." Even with meticulous test implementation, however, it is the stipulation of a single flaw population that seems to cause the most difficulty in using Weibull statistics in dental material strength testing.

In Eq. (1), the parameter Y distinguishes different types of flaws as well as different test specimen test configurations. A blunt flaw, such as a pore, is more benign than a sharp flaw, such as a microcrack. A material under load may break from a sharp flaw but not break from a blunt flaw of a similar size. Suppose a material contains the two flaw types, small microcracks and large pores. Each flaw type has its own distribution. If all the test specimens break from microcracks, or all the test specimens break from pores, then either the microcrack size distribution or the pore size distribution will govern the strength distribution. If, however, some test specimens break from microcracks, and other test specimens break from pores, the strength distributions resulting from the different flaw populations overlap and an associated extreme value distribution cannot be modeled by one single flaw size distribution tail. In this case, the Weibull strength distribution would not be expected to appear smoothly continuous. If many test specimens are tested and enough of them break from either flaw population, parts of *two* distinct Weibull distributions may be discernable. Censored statistical analyses must be used in such cases [32]. Bends or kinks in a Weibull distribution function are often indicative of fracture resulting from multiple flaw types.

Thus, lack of a good Weibull fit is suggestive of an inconsistent underlying flaw population, assuming the material was tested properly and failed in a brittle manner. Conversely, a good Weibull fit is sometimes taken as indicative of a single, dominant flaw type and confirmation of adequate care in testing procedures. Unless material familiarity and previous testing dictates otherwise, it is prudent to verify the cause of fracture initiation. This is often done fractographically and is encouraged, and in cases required, by the standards for Weibull analyses [32–35]. There even are guidelines and formal standards for fractographic analysis that have been prepared with Weibull analysis in mind [31,38].

Another consideration in using Weibull statistics is the increased number of test specimens that might be needed to characterize an entire strength distribution rather than simply estimate a mean strength value. The optimal number of test specimens depends on many variables, including material and testing costs, the values of the distribution parameters and the desired precision for an intended application. Helpful calculations and tables to make such decisions can be found in the previously cited standards. In the absence of specific requirements, a general rule-of-thumb is that approximately 30 test specimens provide adequate Weibull strength distribution parameters, with more test specimens contributing little towards better uncertainty estimates [39–41]. More information regarding optimal test specimen numbers, as well as reasons why Weibull distributions are so often observed in material testing practice are discussed by Danzer et al. [19]. They also detail conditions necessary to obtain a Weibull distribution and suggest alternative statistical approaches for analyzing strength data for materials that do not satisfy these conditions, such as materials with unusual or highly mixed flaw distributions. In this sense, Weibull analysis can be regarded as a special, simple case of a broader statistical approach for analyzing strength data [18–20]. Indeed, Danzer now uses the expression "Weibull material" as one with a single flaw type whose size distribution fits a power law function on the right side tail.

The previous paragraphs highlight some of the assumptions and difficulties in utilizing Weibull statistics in characterizing strength measurements of dental materials. What are the benefits?

It was initially noted that extreme value statistics can be used to predict changes in distributions according to the physical size of the individual test specimens. This is one of the strongest virtues of the Weibull model and what distinguishes it from other distributions. In practical terms, this means that
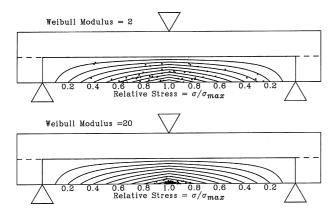
Fig. 3 – A computer generated simulation showing the spread in failure locations (the dots) for 50 flexural strength bars loaded in 3-point loading as a function of Weibull modulus. The arced lines show loci of constant tensile stresses. Fracture origins cluster around the highest stressed areas for materials with large Weibull moduli, but can occur over a broad region for materials with low Weibull moduli (from Johnson and Tucker [42]).

strength values for one test specimen size may be "scaled" to expected strength values for different sized test specimens. This strength scaling permits comparison of strengths of structures with stress gradients such as bend bars or flexed disks. Examples of strength scaling are shown later in this paper. So far we have assumed that all flaws in a body are exposed to the same tensile stresses, but in bodies with stress gradients, some large flaws may be in a low tensile stress or compression region and will not cause fracture. Fracture occurs where there is a critically loaded flaw that has a size, c, and shape factor Y, and a local stress, σ, combination such that the critical fracture toughness, K_{Ic}, is reached in accordance with eq. (1).[1] Fig. 3 by Johnson and Tucker [42] illustrates how fracture origin sites may be scattered in a 3-point bend bar. For materials with low Weibull moduli (i.e., the flaw sizes are quite variable) fracture can occur from a large portion of the test specimen. On the other hand, the origin sites are concentrated to only the highest stressed regions if the Weibull modulus is large, since the flaw sizes are all similar.

The validity of the Weibull approach can be tested by its ability to scale strengths for a particular specimen size to another size or testing configuration. A review of ceramic flexural strength data [43] tabulated a number of studies wherein ceramic strength scaling by Weibull analysis was successful over a size range as much as four orders of magnitude in volume or area! Strength scaling is done by the concept of an "equivalent" volume or area under stress, discussed in a following section. Whether equivalent volumes or equivalent areas are used depends on whether fracture initiates from volume flaws or surface flaws within the stressed region.[2] Using

Weibull statistics to calculate corresponding strengths for different test specimen sizes, test specimen shapes and stress configurations is particularly appealing for use in the dental field where sample sizes and testing configurations are frequently different.

Identification and quantization of different flaw populations can explain strength differences and ultimately lead to improved materials. Such approaches can, for example, isolate the effects of grinding media and surface treatments, or determine whether strength might be improved by reducing porosity. Most important of all, determination of the dominant flaw populations, the effects of stress configurations and physical size are all necessary for correlations to clinical components.

3. Experimental examples and discussion

As noted above in Eq. (2), three parameters were used to define the previously introduced extreme value functions, but only two Weibull parameters are generally reported for strengths. The two-parameter Weibull distribution is obtained by setting $\sigma_u = 0$, although the three parameter form is not uncommon. When the three parameter Weibull distribution is used, the lower strength bound, σ_u, might represent a lower strength limit for a data set. This is analogous to a data set that may have been previously proof-tested or inspected to eliminate flaws over a certain size. The lower bound strength could also correspond to a physical limit to a crack size. It is very risky to assume a finite threshold strength exists without careful screening or nondestructive evaluation. Hence, the two-parameter form is most commonly used for simplicity.

Setting σ_u to zero in Eq. (2) and taking the double logarithm of the resulting two-parameter Weibull distribution yields:

$$P_f = 1 - \exp\left(-\left(\frac{\sigma}{\sigma_\theta}\right)^m\right)$$

$$\ln(1 - P_f) = -\left(\frac{\sigma}{\sigma_\theta}\right)^m$$

$$\ln\left[\ln\left(\frac{1}{1-P_f}\right)\right] = m\ln\sigma - m\ln\sigma_\theta \tag{3}$$

The reason the double logarithm of the Weibull equation is used in strength analysis is the ease of accessing information. Appendix A shows how Eq. (3) yields the Weibull parameters in a simple graphical representation of the data with a slope of the Weibull modulus, m. Fig. 4 shows an example for alumina. One can perform a simple linear regression analysis to get the Weibull parameters, but many analysts prefer the maximum likelihood estimation approach as discussed in Appendix. The characteristic strength, σ_θ, is a location parameter; a large σ_θ shifts the data to the right, while a small σ_θ shifts the data to the left. The characteristic strength is the strength value, σ, at $P_f = 63.2\%$, when the left side of Eq. (3) = 0. Thus reported Weibull characteristic strength values ($P_f = 63.2\%$) are slightly greater than the mean strength values ($P_f = 50\%$).

The double logarithm of the reciprocal $(1 - P_f)$ on the left side of Eq. (3) explains the unusual interval spacing of the

---

[1] For simplicity, we ignore rising R-curve behavior whereby fracture resistance changes with crack size and we also ignore environmentally assisted slow crack growth.

[2] In rare instances, strength is controlled by edge origin sites, and strength scales with the effective edge lengths.
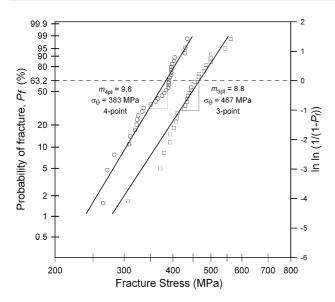
Fig. 4 – Weibull plots of alumina bars broken in flexure using 3-point (□) and 4-point (○) test configurations. The bars broken in 3-point flexure broke at greater stresses. The parallel shift to the right of the whole distribution is predicted by Weibull theory. The Weibull parameters and fitted lines are from maximum likelihood analysis.

P_f labels on the ordinate (y) axis of the Weibull graph. Two examples are used in this section to illustrate the previous concepts. The example in Appendix A also illustrates some of these topics.

3.1. Example 1: alumina 3- and 4-point flexure tests

This first example illustrates strength differences in polycrystalline alumina bars tested in 3-point and 4-point flexure. The bar sizes were all 3 mm × 4 mm × 50 mm. The 3-point flexure test specimens had 40 mm outer spans, and the 4-point flexure test specimens had 40 mm outer spans and 20 mm inner spans. Stresses were calculated by the formulae [44]:

$$\sigma_{3\text{-pt}} = \frac{3PL}{2bd^2} \quad \text{for the 3-point flexure tests}$$

$$\sigma_{4\text{-pt}} = \frac{3PL}{4bd^2} \quad \text{for the 1/4-point, 4-point flexure configuration}$$

where P is the break load, L is the outer span length, b is the test specimen width, and d is the test specimen height. The 1/4-point qualifier for the 4-point configuration means that the inner loading rollers are located inward by $1/4L$ from the outer loading rollers.

For each of the two test configurations, the stress values were ranked in ascending order, $i = 1, 2, 3, \ldots, N$, where N is the total number of test specimens and i is the ith datum. Thus, the lowest stress for each configuration represents the first value ($i = 1$), the next lowest stress value is the second datum ($i = 2$), etc., and the highest stress is represented by the Nth datum. This enables a ranked probability of failure, $P_f(\sigma_i)$, to

be assigned to each datum according to

$$P_f(\sigma_i) = \frac{i - 0.5}{N} \tag{4}$$

Although there are other formulations to assign failure probabilities, the one shown in Eq. (4) is widely used and has negligible bias as discussed in Appendix.

Since the fracture stress and the associated P_f for each datum are now known, a graph may be constructed using the left side of Eq. (3) on the ordinate and $\ln(\sigma)$ on the abscissa. This comprises Fig. 4, where the 3-point flexure bar data (squares) are at the right, at higher strengths, than the 4-point flexure bar data (circles). There are two common approaches to fit a line through the data: linear regression analysis and maximum likelihood estimation analysis [45–48]. The pros and cons of each analysis are described in more detail in the Appendix, but, as mentioned above, most world standards use the latter. The MLE analysis was used for the Weibull parameter estimates in Fig. 4 and Table 1. The strength difference for the same material seems large, but this is to be expected according to weakest link theory, as more material is under higher stress in the 4-point configuration, with a higher probability of containing a larger flaw.

It can be seen from Fig. 4 that the slopes (Weibull moduli) indicate the strength distribution widths. The similar slopes suggest that the same flaw types were active in both specimen sets and this indeed was verified by fractographic analysis. The wriggles in the curves are not unusual and are common in small size sample sets. A high modulus, or steep slope, is associated with a narrow strength distribution. This is usually desirable, as materials with high Weibull moduli are more predictable and less likely to break at a stress much lower than a mean value. The characteristic strength, or Weibull scale parameter σ_θ, indicates the distribution location along the abscissa (x) axis, and is expected to move according to test specimen size or the amount of material that is highly stressed. Thus, the distributions for 3- and 4-point flexure are expected to have the same shape (m value), but move to the right (higher σ_θ value) as test specimen sizes or stressed volumes decrease. This is directly analogous to the "march" of the "largest flaw" distribution presented in a previous section. It was also stated in previous sections that such measured strength changes due to differences in test specimen size and configuration can be quantitatively predicted using Weibull parameters. This can be accomplished through the concept of equivalent areas or volumes.

3.2. 3-Point and 4-point flexural strength comparisons using equivalent volumes

Fractographic analysis of the flexure test specimens graphed in Fig. 4 determined the predominant flaw type was volume-distributed porosity or agglomerates associated with porosity. Inclusions caused fracture in some test specimens, and the flaw mix probably contributed to some of the wriggles in Fig. 4 data. Since the flaws were volume distributed, we will compare the two data sets using an equivalent volume approach. In the Weibull weakest link model, the size-strength relation-

Material (number of specimens)	Flexure test type	Mean strength (std. dev.)	Weibull char. strength, σ_θ (90% conf. interval)	Weibull modulus, m (90% conf. interval)
Alumina (32)	4-point, 40 mm × 20 mm spans	364(45) MPa	383(370–396) MPa	9.6 (7.3–11.7)
Alumina (30)	3-point, 40 mm span	444(51) MPa	467(449–485) MPa	8.8 (6.6–10.7)
Porcelain 1 (27)	4-point, 20 mm × 40 mm spans	84.7 (5.3) MPa	87.1 (85.4–88.8) MPa	18.5 (13.6–22.7)
Porcelain 2 (26)	4-point, 10 mm × 20 mm spans	112(8) MPa	115(113–118) MPa	18.0 (13.1–22.2)

Table 1 – Strength tests with different flexural configurations and maximum likelihood estimates of the Weibull parameters.

ship can be expressed [43,46–48]:

$$\frac{\sigma_1}{\sigma_2} = \left(\frac{V_{E2}}{V_{E1}}\right)^{1/m} \tag{5}$$

where m is the Weibull modulus, σ_1 and σ_2 are the mean (or median or characteristic) strengths of test specimens of type 1 and 2 which may have different sizes and stress distributions, and V_{E1} and V_{E2} are the associated effective volumes. (Effective areas may be substituted for the effective volumes in Eq. (5) for surface flaws, such as machining damage.) A unimodal flaw population that is uniformly distributed throughout the volume and a Weibull two-parameter distribution are assumed.

The effective volume approach is illustrated in Fig. 5. In the simplest case of direct uniform tension, V_E is the test specimen volume, V. Many test specimens or components such as flexural loaded rods or bars have stress gradients and $V_E < V$. Sometimes the relationship between the two is expressed as $V_E = KV$, where K is called the loading factor and is dimensionless and V is the total volume within the outer loading points. As shown in Fig. 5, V_E is the volume of a hypothetical tensile test specimen, which when subjected to the stress $\sigma_{\max}$, has the same probability of fracture as the flexure test specimen stressed at $\sigma_{\max}$. In other words, a flexure bar of volume V is equivalent to a tensile test specimen of size V_E. K is 1 for an ideally loaded tension specimen. K is typically less than 1
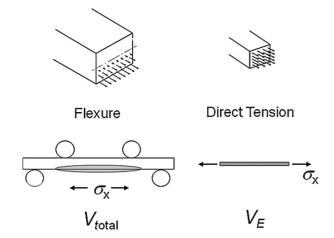

Fig. 5 – The concept of equivalent volume. σ_x shows the direction of the tensile stresses. Only part of the total volume, V, of the flexure specimen on the left is in tension. Only a smaller fraction of this region (depicted by the shaded area) is exposed to large tension stresses. An equivalent direct tension specimen with the same effective volume, V_E, is shown on the right. How much of the flexure specimen volume should be counted depends on the Weibull modulus.

for parts or test specimens that have stress gradients, i.e., the stress varies with position within the body.

Equations for effective volumes and effective areas may be determined from knowledge of the stress state, or looked up in the literature for common configurations, such as flexure of rectangular bars [49] or round rods [50]. For the flexure bars in Fig. 4, the effective volumes can be calculated:

V_E of the 1/4-point 4-point flexure test specimen

$$= \frac{(L_o b d)(m + 2)}{[4(m + 1)^2]}$$

V_E of the 3-point flexure test specimens $= \frac{(L_o b d)}{[2(m + 1)^2]}$

where L_o is the outer span length, b is the test specimen width, d is the test specimen height, and m is the Weibull modulus. In other words, the effective volumes are equal to the specimen volume ($L_o b d$) within the loading span multiplied by a dimensionless term including the Weibull modulus. The latter term takes into account the stress gradient, but also reflects the influence of the variability in flaw sizes. The portions of the test specimen that lie beyond the fixture outer span are unstressed and do not contribute to the effective volumes. The same is true of the portions stressed in compression. In our example, the flexure bars all have the same outer span length of 40 mm, and same height and width of 3 and 4 mm, respectively. The ratio of effective volumes is thus

$$\frac{V_{E4-pt}}{V_{E3-pt}} = \frac{m + 2}{2}$$

This can be substituted into Eq. (5) to yield a simple expression for determining the expected strength ratio for the 3- and 4-point flexure test configurations:

$$\sigma_{3\text{-pt}} = \sigma_{4\text{-pt}} \left(\frac{V_{E4-pt}}{V_{E3-pt}}\right)^{1/m} = \sigma_{4\text{-pt}} \left[\frac{m + 2}{2}\right]^{1/m}$$

Using an average m of 9.2, the 3-point strengths should be 1.206 times the 4-point strengths, in excellent agreement with the experimentally determined ratio of 1.216. In other words, the 3-point strengths are 21% stronger than the 4-point strengths, in good agreement with the prediction. This example demonstrates how the Weibull function can be utilized to predict the scaling of strengths to other configurations.

3.3. Example 2: comparison of two porcelains using different sized flexure bars

In this second example, the strengths of two different porcelains, Porcelain 1 and Porcelain 2 are compared. Both are feldspathic porcelains containing well-dispersed crystallites of similar sizes. The porcelains differ, however, in crystalline
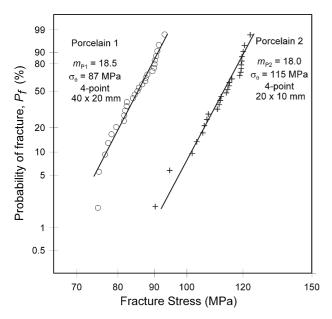
Fig. 6 – Weibull plots of two feldspathic porcelains tested in different configurations. The Weibull parameters are from maximum likelihood analysis. The Weibull moduli are similar, and the specimens tested with the shorter span broke at higher stresses. Is this difference expected if the two materials have similar strengths?

volume content and crystalline phases, and were obtained from different manufacturers. Porcelain 1 and Porcelain 2 both had cross-sections of $3\,mm \times 4\,mm$ and both were tested in 1/4-point, 4-point flexure. The Porcelain 2 test specimens were shorter than the Porcelain 1 test specimens, however, and were tested using shorter spans. Porcelain 2 was tested with a 20 mm outer span and 10 mm inner span. The longer Porcelain 1 test specimens were tested with the same fixture design, but with a 40 mm outer span and 20 mm inner span.

As in the previous example, the data were ranked and each datum was assigned a failure probability and then graphed using Eq. (3). The results are shown in Fig. 6 and Table 1. The slopes are very similar (18.5 and 18.0), and the shorter test specimens had higher strengths, as would be expected from weakest link theory. Are the test specimens truly comparable in terms of strength? If Porcelain 2 were tested in $40\,mm \times 20\,mm$ fixtures instead of the smaller $20\,mm \times 10\,mm$ fixtures, would the strengths be similar to Porcelain 1?

Fractographic examination of the materials plotted in Fig. 6 indicated that the two porcelains generally failed from intrinsic flaws that were volume distributed. Once again we return to Eq. (5). In this case we need the effective volume ratio for longer and shorter test specimens tested in 4-point flexure. Again using the equation for 1/4 4-point flexure:

$$V_E = \frac{(L_o bd)(m+2)}{[4(m+1)^2]}$$

Since all the quantities in the previous equation are the same for the two porcelains except the span lengths, the effective

volume ratio is simply:

$$\frac{V_{E\ small\ span}}{V_{E\ large\ span}} = \frac{20\,mm}{40\,mm} = 0.5$$

The Weibull modulus of Porcelain 2 is 18.0. Thus, from Eq. (4):

$$\sigma_{P2\ large\ span} = \left(\frac{20}{40}\right)^{1/18} \sigma_{P2\ small\ span} = 0.96\sigma_{P2\ small\ span}$$

The expected strength of Porcelain 2, if the test specimens were longer and tested with 40 mm spans, is only 4% less. The small difference is due to the large Weibull modulus so that the effective volumes are not vastly different. Although Weibull scaling predicts a 4% difference in strength if Porcelain 2 was tested with longer spans, the measured difference in strengths of the two porcelains would be much greater—about 25%. Utilizing the tables in Ref. [41] and ASTM C1239 [32], the high moduli and adequate numbers of test specimens for both configurations result in 90% confidence bounds that are sufficiently narrow to indicate the porcelain strengths are statistically significantly different. Porcelain 2 has a higher calculated strength than Porcelain 1 for a similar test configuration.

3.4. Example 3: Deviations from a unimodal strength distribution in a zirconia

Fig. 7 shows an example where a single Weibull distribution is a poor fit. Thirty nine commercial 3Y-TZP zirconia bend bars of size $3\,mm \times 4\,mm \times 45\,mm$ were tested on $20\,mm \times 40\,mm$ 4-point fixtures. Fractographic analysis was done on every test specimen and revealed that most of the strength limiting flaws were volume-distributed pores between 10 and 20 μm in diameter. The six weakest specimens broke from unusually large flaws such as compositional inhomogeneities, inclusions, and gross pores, so it is not surprising that the strength trend is irregular. A proper analysis of this data set would require the use of censored statistical analyses as described in [32]. In this example, the low strength tail of the distribution was readily apparent since a large number of test specimens were available. Had only 10 or 15 specimens been broken, then it is possible that only one or two weak specimens would have been revealed and the low strength problem not detected.

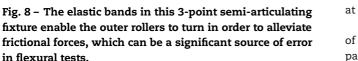### 3.5. Additional considerations and assumptions

The previous examples demonstrate some of the problems and advantages of using Weibull statistics. A single flaw population is assumed and should be verified, test specimen numbers should be sufficient to determine the Weibull parameters within acceptable confidence bounds, and the calculations and results are more cumbersome than simple determination of a mean stress value. On the other hand, it was possible to quantitatively compare expected strengths for the different materials and test configurations, as well as peruse the plots for an idea of the comparative distribution widths.

As a final note, it should be mentioned that all the test specimens were tested using self-aligning fixtures with rollers, such as shown in Fig. 8. The elastic bands in the figure apply

Fig. 7 – Flexural strength of 3Y-TZP zirconia bend bars. The maximum likelihood fitted line is a poor fit to the distribution. Although most specimens had pore origins like the one shown on the upper insert, the six weakest test specimens had atypical flaws such as the one shown on the lower left.

enough force to keep the rollers in place while allowing them to rotate when a flexure load is applied. The allowed rotation is quite important, for the supports and load points will be subject to a frictional force if the rollers are not free to roll. The errors due to friction are significant, but almost always ignored in the dental literature, where frictionless load points are assumed in the calculations. Experimental differences in failure stress using rigid knife edges as compared to roller-type contact points have been measured higher than 11% [51–53]. The frictional force prevents the load points from rolling apart, and superimposes a compressive force on the tensile face of the test specimen. Thus, the error results in apparently "stronger" test specimens than would result from rolling sup-

Fig. 8 – The elastic bands in this 3-point semi-articulating fixture enable the outer rollers to turn in order to alleviate frictional forces, which can be a significant source of error in flexural tests.

ports. Significant errors can also result from misalignment, especially if the bars are not of constant geometry or flat and parallel [43,54,55]. No amount of statistical manipulation can compensate for indiscriminate test procedures.

4. Conclusion

There is a strong theoretical foundation for Weibull statistical analysis of strength data based on extreme value theory, fracture mechanics, and demonstrated flaw size distributions. However, awareness of the conditions and limitations inherent in Weibull analyses, especially those pertaining to existing flaw populations and quality of data, is important for meaningful application and interpretation. A great deal of useful information is available through Weibull analysis. Among the most useful applications are comparisons of strength values and ranges for different stress configurations, which were demonstrated in Section 3 for several dental materials.

Acknowledgements

Appendix A.

How to prepare a Weibull strength distribution graph

The following example utilizes fictitious data in order to demonstrate how a Weibull strength distribution graph is prepared. Suppose that five test specimens produce strength outcomes of: 255, 300, 330, 295, and 315 MPa. More than 5 data are advisable for most conditions and this small sample set is for illustrative purposes only. The first step is to order the data from lowest to highest strengths as shown in the second column of Table A1.

The natural logarithms of the stresses are computed and shown in the third column. These values will be plotted along the horizontal axis of a Weibull graph.

Next, a cumulative probability of fracture, P_f, is estimated and assigned to each datum. A commonly used estimator that has low bias when used with linear regression analyses is $P_f = (i - 0.5)/n$, where i is the ith datum and n is the total number of data points. This is the estimator used in the main text. Many studies (e.g. [A1–A4,45]) have shown that for $n > 20$, this estimator produces the least biased estimates of the Weibull parameters. Using the estimator for the first ($i = 1$) data point out of $n = 5$ total points, P_f is estimated to be 0.10% or 10% as shown in the fourth column of Table A1. This means that if many test specimens were broken, it is estimated that 10% of all outcomes would be weaker than the specimen that broke at a stress of 255 MPa. 90% would be stronger.

The next step is to compute the double natural logarithm of $[1/(1 - P_f)]$ in accordance with Eq. (3) in the main body of the paper. This is listed in the last column of the table.
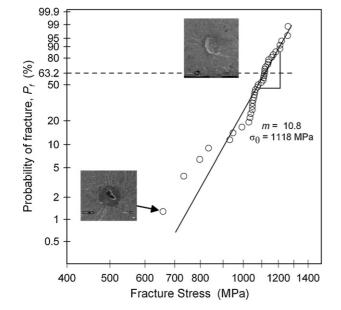
i	Strength (MPa)	$X = \ln(\text{strength})$	$P_f = (i - 0.5)/n$	$Y = \ln \ln [1/(1 - P_f)]$
	Table A1 – Example data set for 5 test specimens.			
1	255	5.5413	0.10	−2.2504
2	295	5.6870	0.30	−1.0309
3	300	5.7038	0.50	−0.3665
4	315	5.7526	0.70	0.1856
5	330	5.7991	0.90	0.8240

A graph is prepared with $X = \ln(\text{strength})$ plotted on the horizontal axis, and $Y = \ln \ln[1/(1 - P_f)]$ on the vertical axis. Fig. A1 shows a graph with these two axes shown on the right and top sides. For convenience, the axes are often labeled with the values of fracture stress and P_f, as shown along the left and bottom sides of the graph. Note how the values of these parameters are not simply and evenly distributed along the axes, but stretched according to the logarithmic and double logarithmic functions.

Finally, a line is fitted through the data. Linear regression (LR) analysis is commonly used since it is the easiest to understand and can be done with a hand calculator, a simple spreadsheet, or many common graphics software programs. The usual procedure is to regress the $\ln \ln[1/(1 - P_f)]$ values onto $\ln(\text{fracture stress})$, or in other words, to minimize the vertical deviations in the graph. The slope of the line is the Weibull modulus, m. The characteristic strength, σ_θ, is the value of stress for which $\ln \ln[1/(1 - P_f)]$ is zero, or $P_f = 63.2\%$. It is analogous to the median strength, except that the latter is at $P_f = 50\%$. The Weibull modulus and characteristic strength from the linear regression analysis are shown on the right of the line in Fig. A1. (Users should be cautioned that some algorithms and computer programs regress the opposite way, so that *horizontal* deviations are minimized. Different Weibull parameter estimates are obtained.)

The Weibull modulus and characteristic strength from linear regression analysis are adequate for many cases, but it should be borne in mind that these are estimates. The confidence bounds or uncertainties on these estimates may be obtained from the literature. In general, estimates of the characteristic strength quickly converge to population values as the number of specimens is increased to ten or more. On the other hand, Weibull modulus estimates can be quite variable for a sample set with only a small number of test specimens or if the data do not fall on a single line. Therefore, it is common to require no fewer than ten test specimens and preferably 30 to obtain good estimates of the Weibull modulus.

The literature includes many papers suggesting new and improved P_f estimators for linear regression analyses. There are far too many to list here. Usually Monte Carlo simulations with an assumed Weibull distribution generate many small data sets which are analyzed in turn by the chosen linear regression scheme. Scatter in the computed Weibull parameters as well as bias trends (the parameters on average do not match the assumed parent distribution) are analyzed and compared to results when using the usual $P_f = (i - 0.5)/n$ estimator. Ideally, the results should have low scatter (tight confidence bounds) and negligible bias. Some of the proposed estimators are quite implausible, however. For example, one study suggested the use of $P_f = (i - 0.999)/(n + 1000)$ [A5]. So for a set of 30 specimens, this estimator suggests the first strength datum corresponds to a $P_f = 1.0 \times 10^{-4}\%$, and, for the last datum, a $P_f = 28\%$. It is unreasonable to assume that the weakest data point of a set of 30 specimens gives useful information about a probability of fracture of one part in 10,000. With the traditional $P_f = (i - .5)/n$, one obtains far more plausible estimates of 1.7% and 98.3%. These numbers mean that one might expect only 1.7% of additional test strengths would be weaker than the first datum and 98.3% would be weaker than the strongest recorded test outcome. Two subsequent papers showed that dramatic correction factors for bias had to be used when using the $P_f = (i - 0.999)/(n + 1000)$ estimator [A6,A7]. For most Weibull analyses, it is not necessary to resort to such exotic probability estimators and, as stated above, leading researchers [45–48,A1–A4] have concluded that for $n > 20$, the $P_f = (i - .5)/n$ estimator gives parameters estimates with small bias and reasonable confidence limits. Users should be cautious with smaller sample sets than 10, however, since bias in the Weibull modulus can be 5% or more [45,A1–A4,A8,A9].

An important and common alternative analysis to fit the data is the Maximum Likelihood Estimation (MLE) approach. It is a more advanced analysis that is preferred by many statisticians since the 90% or 95% confidence intervals on the estimates of the Weibull parameters are appreciably tighter than those from linear regression [42,45,A4,A5,A9]. Furthermore, it is not necessary to use a probability estimator for P_f.
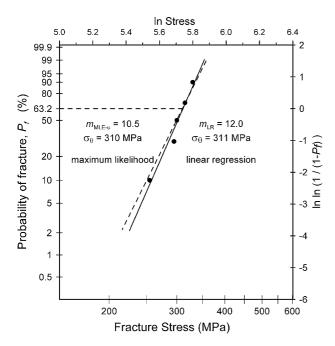

Fig. A1 – Weibull graph for the Table A1 data set. The linear regression and maximum likelihood estimator lines and Weibull parameter estimates are shown for comparison.

For these reasons, MLE is incorporated into the comprehensive Weibull standards for analysis of strength data [32–35] which all give identical Weibull parameter estimates and confidence bounds for a particular data set. MLE analysis is strongly preferred for design. MLE analysis, which is explained well in Ref. [46], estimates the Weibull parameters by maximizing a likelihood function. The MLE analysis is usually described in mathematical terms (e.g. [45–48]), but a simplified description of how it works is as follows. A first estimate, or "guess" is made of the Weibull parameters and, for each actual test strength outcome, a probability of occurrence is calculated. For a given test set of say $n = 30$ strengths, the probabilities are summed. Another slightly different Weibull distribution, with different modulus and characteristic strength, is then tried and the probabilities are also summed. The Weibull parameters are iteratively adjusted until the optimum, or "most likely," parameters are found to fit the actual test data. This iterative analysis is typically done with a computer program.[3] The MLE estimate for the characteristic strength has negligible bias, but a small correction factor is usually applied to correct or "unbias" the Weibull modulus estimate [32–35,41]. Users of MLE programs should check whether or not the calculated moduli are corrected for bias. A MLE fitted line is also shown in Fig. A1. In this example, the Weibull MLE and LR parameter estimates are similar. This is commonly the case for the characteristic strength, but MLE and LR estimates of the Weibull modulus usually differ. Linear regression analyses usually "chase the lowest strength data points" whereas MLE seems to "chase the highest strength data points" [48]. One might ask: which is better? The answer is that each gives reasonable estimates of the Weibull modulus, but, since the confidence intervals for the MLE estimates are tighter, statisticians and designers prefer MLE. For more details on the MLE analysis, the reader should consult Refs. [41,46] or the Weibull strength standards [32–35]. With the sole exception of the short annex in the Dental Standard ISO 6782:2008 [36] (which has no information on confidence bounds), all other standards specify strength data analysis by MLE and include instructions on how to determine the confidence bounds.

There are many reasons why strength data may deviate from a straight line when plotted as shown above. A non-zero threshold strength may cause the trend to curve downward at lower strengths. Bends or wriggles in the trend may be a consequence of small sample sizes (e.g. for $n \leq 10$) or may be manifestations of multiple flaw populations. More advanced analyses for bimodal strength distributions are available (e.g. censored statistical analysis as specified in ASTM C 1239 [32] or ISO 20501 [35]). Fractographic analysis may help determine the cause of bends or wriggles in a data set.

---

[3] The actual calculation used by most programs uses a more efficient scheme. The likelihood function is the mathematical product of the probability density function values for a series of experimental strength values. This product (actually the natural logarithm of the product for mathematical convenience) is differentiated twice, once with respect to m, and once with respect to σ_θ. The two differential equations are set equal to zero to find the maximum, i.e., the maximum likelihood. The two nonlinear equations are then are solved iteratively to obtain the maximum likelihood parameter estimates.

REFERENCES

[1] Yeung C, Darvell BW. Fracture statistics of brittle materials—parametric model validity. J Dent Res 2006;85. Spec Iss B, Abstr. No. 1966.
[2] Quinn GD, Quinn JB. Are Weibull statistics appropriate for dental materials? J Dent Res 2005;84 (Spec Iss A), Abstr. No. 1463.
[3] Weibull W. A statistical theory of the strength of materials. Royal Inst for Eng Res, Stockholm 1939;151:1–45.
[4] Abernethy RB. An overview of Weibull analysis. In: The new Weibull handbook. 5th ed. North Palm Beach, FL: Robert B. Abernethy; 2006.
[5] Bannerman DB, Young RT. Some improvements resulting from studies of welded ship failures. Weld J 1946;25(3):223–36.
[6] Wells AA. Conditions for fast fracture in aluminum alloys with particular reference to the Comet failures, vol. 129. BWRA Research Board, RB; 1955.
[7] Anderson TL. Fracture Mechanics. 2nd ed. New York, NY: CRC Press; 1995.
[8] Griffith AA. The phenomenon of rupture and flow in solids. Philos Trans R Soc 1921;A221:163–98.
[9] Irwin GR. Onset of fast crack propagation in high strength steel and aluminum alloys. In: Proceedings of the Sagamore Research Conference, vol. 2. Syracuse University Press; 1956, 289–305.
[10] Lund JR, Byrne JP. Leonardo DaVinci's tensile strength tests: implications for the discovery of engineering mechanics. Civil Eng Environ Syst 2000;00:1–8.
[11] Kotz S, Nadarajian S. Extreme value distributions: theory and applications. London: Imperial College Press; 2000.
[12] Fisher RA, Tippet LH. Limiting forms of the frequency distribution of the largest or smallest member of a sample. Proc Camb Phil Soc 1928;24:180–90.
[13] Ledermann W, Lloyd E, Vajda S, Alexander C. Extreme value theory, chapter 14 in Handbook of Applicable Mathematics. New York: Wiley; 1980.
[14] NIST/SEMATECH e-Handbook of statistical methods, http://www.itl.nist.gov/div898/handbook/, June 2007.
[15] Weibull W. A statistical distribution function of wide applicability. J Appl Mech 1951;(September):293–7.
[16] Jayatilaka ADES, Trustrum K. Statistical approach to brittle fracture. J Mater Sci 1977;12:1426–30.
[17] Trustrum K, Jayatilaka ADeS. Applicability of Weibull analysis for brittle materials. J Mater Sci 1983;18: 2765–70.
[18] Danzer R. A general strength distribution function for brittle materials. J Eur Ceram Soc 1992;10:461–72.
[19] Danzer R, Lube T, Supanic P, Damani R. Fracture of ceramics. Adv Eng Mater 2008;10(4):275–98.
[20] Lu C, Danzer R, Fischer FD. Fracture statistics of brittle materials: Weibull or normal distribution. Phys Rev E 2002;65, article 067102.
[21] Abe H, Naito M, Hotta T, Shinohara N, Uematsu K. Flaw size distribution in high quality alumina. J Am Ceram Soc 2003;86(6):1019–21.
[22] Bakas MP, Greenhut VA, Niesz DE, Quinn GD, McCauley JW, Wereszczak AA, et al. Anomalous defects and dynamic failure of armor ceramics. Int J Appl Ceram Tech 2004;1(2):211–8.
[23] Zhang Y, Inoue N, Uchida N, Uematsu K. Characterization of processing pores and their relevance to the strength of alumina ceramics. J Mater Res 1999;14(8):3370–4.
[24] Flashner F, Zewi IG, Kenig S. Fractography and Weibull distribution relationship in optical fibres. Fibre Sci Tech 1983;19(4):311–5.

[25] Dusza J, Steen M. Fractography and fracture mechanics property assessment of advanced structural ceramics. Inter Mater Rev 1999;44(5):165–216.

[26] Boyce BL, Grazier MJ, Buchheit TE, Shaw MJ. Strength distributions in polycrystalline silicon MEMS. J Microelectromech Syst 2007;16(2):179–90.

[27] Della Bona A, Mecholsky JJ, Anusavice KJ. Fracture behavior of lithia disilicate- and leucite-based ceramics. Dent Mater 2004;20(10):956–62.

[28] Wolf WD, Vaidya KJ, Falter Francis L. Mechanical properties and failure analysis of alumina-glass dental composites. J Am Ceram Soc 1996;79(7):1769–76.

[29] Lüthy H, Filser F, Loeffel O, Schumacher M, Gauckler LJ, Hammerle CHF. Strength and reliability of four-unit all-ceramic posterior bridges. Dent Mater 2005;21:930–7.

[30] Rice RW. Ceramic fracture features, observations, mechanisms, and uses. In: Mecholsky Jr JJ, Powell Jr SR, editors. Fractography of ceramic and metal failures. West Conshohocken, PA: ASTM STP 827, ASTM Int; 1984. p. 5–103.

[31] Quinn GD. Fractography of ceramics and glasses. NIST Recommended Practice Guide, Sp. Pub. 960-16. Gaithersburg, MD: U.S. Dept. of Commerce; 2007.

[32] ASTM C1239. Standard practice for reporting strength data and estimating Weibull distribution parameters for advanced ceramics. West Conshohocken, PA, USA: ASTM Int.; 1995.

[33] JIS R1625. Weibull statistics of strength data for fine ceramics. Tokyo, Japan: Japanese Industrial Standards Association; 1996.

[34] BS EN 843-5. Advanced technical ceramics–Mechanical properties of monolithic ceramics at room temperature. Part 5: Statistical analysis. London, UK: British Standard Institute; 2006.

[35] ISO 20501. Weibull statistics for strength data. Geneva, Switzerland: International Organization for Standards; 2003.

[36] ISO 6872. Dentistry–ceramic materials. Geneva, Switzerland: International Organization for Standards; 2008.

[37] Reliability of Ceramics for Heat Engine Applications, National Materials Advisory Board Report 357, National Academy of Sciences, Washington, DC (1980).

[38] ASTM C 1322. Standard practice for fractography and characterization of fracture origins in advanced ceramics. West Conshohocken, PA: ASTM Int; 1996.

[39] Ritter JE, Bandyopadhyay N, Jakus K. Statistical reproducibility of the dynamic and static fatigue experiments. Ceram Bull 1981;60(8):798–806.

[40] Johnson CA, Tucker WT. Advanced statistical concepts of fracture in brittle materials, in Ceramic Technology for Advanced Heat Engines Project, semiannual progress report for October 1990 through March 1991, Oak Ridge National Laboratories Report TM-11859, 1991; pp. 268–82.

[41] Thoman DR, Bain LJ, Antle CE. Inferences on the parameters of the Weibull distribution. Technometrics 1969;11(3):445–60.

[42] Johnson CA, Tucker WT. Advanced statistical concepts of fracture in brittle materials. In: Proceedings of the twenty-third automotive development contractor's coordination meeting, Report P-165, vol. 1086. 1956. p. 265–9.

[43] Quinn GD, Morrell R. Design-data for engineering ceramics—a review of the flexure test. J Am Ceram Soc 1991;74(9):2037–66.

[44] ASTM C1161. Standard test method for flexural strength of advanced ceramics at ambient temperature. West Conshohocken, PA, USA: ASTM Int; 2002.

[45] Trustrum K, Jayatilaka ADeS. On estimating the Weibull modulus for a brittle material. J Mater Sci 1979;14:1080–4.

[46] Wachtman JB, Cannon WR, Mattewson MJ. Mechanical properties of ceramics. 2nd ed. NY: Wiley; 2009.

[47] Munz D, Fett T. Ceramics, mechanical properties, failure behavior, materials selection. Berlin: Springer-Verlag; 2001.

[48] Davies DGS. The statistical approach to engineering design in ceramics. Proc Br Ceram Soc 1973;22:429–52.

[49] Quinn GD. Weibull strength scaling for standardized rectangular flexure specimens. J Am Ceram Soc 2003;86(3):508–10.

[50] Quinn GD. Weibull effective volumes and surfaces for cylindrical rods loaded in flexure. J Am Ceram Soc 2003;86(3):475–9.

[51] Newnham RC. Strength tests for brittle materials. Proc Br Ceram Soc 1975;25:281–93.

[52] Weil NA. Studies of brittle behavior of ceramic materials. U.S. Air Force technical report ASD TR 61-628, Part II: 38–42, Wright Paterson Air Force Base, Dayton, OH, 1962.

[53] Quinn GD. Twisting and friction errors in flexure testing. Ceram Eng Sci Proc 1992;13(7–8):319–30.

[54] Baratta FI, Quinn GD, Matthews WT. Errors associated with flexure testing of brittle materials. MTL TR 87-35. Watertown, MA: U.S. Army Materials Technology Laboratory; 1987.

[55] Hoagland RG, Marschall CW, Duckworth WH. Reduction of errors in ceramic bend tests. J Am Ceram Soc 1976;59(5–6):189–92.

Appendix references

[A1] Bergman B. On the estimation of the Weibull modulus. J Mater Sci Lett 1984;3:689–92.

[A2] Sullivan JD, Lauzen PH. Experimental probability estimators for Weibull plots. J Mater Sci Lett 1986;15:1245–7.

[A3] Steen M, Sinnema S, Bressers J. Statistical analysis of bend strength data according to different evaluation methods. J Eur Ceram Soc 1992;9:437–45.

[A4] Langlois R. Estimation of Weibull parameters. J Mater Sci Lett 1991;10:1049–51.

[A5] Gong J. A new probability index for estimating Weibull modulus for ceramics with the least-square method. J Mater Sci Lett 2000;19:827–9.

[A6] Wu D, Jiang H. Comment on: a new probability index for estimating Weibull modulus for ceramics with the least-square method. J Mater Sci Lett 2003;22:1745–6.

[A7] Griggs JA, Zhang Y. Determining the confidence intervals of Weibull parameters estimated using a more precise probability estimator. J Mater Sci Lett 2003;22:1771–3.

[A8] Tiryaklioglu M. An unbiased probability estimator to determine Weibull modulus by the linear regression method. J Mater Sci 2006;41:5011–3.

[A9] Khalili K, Kromp K. Statistical properties of Weibull estimators. J Mater Sci 1991;26:6741–52.